Japanese Journal of Applied Physics
Vol. 46, No. 9B, 2007, pp. 6324–6328
©2007 The Japan Society of Applied Physics

Mechanical Properties of Single Carbon Nanofibers Grown on Tips of Scanning Probe Microscopy Cantilevers by Ion Irradiation

Masashi KITAZAWA[1,2]*, Ryo OHTA[1], Tatsuhiko OKITA[2], Junya TANAKA[2], and Masaki TANEMURA[2]

[1]*Olympus Co., Ltd., Tatsuno, Nagano 399-0495, Japan*
[2]*Department of Environmental Technology, Graduate School of Engineering, Nagoya Institute of Technology, Nagoya 466-8555, Japan*

(Received October 25, 2006; accepted April 16, 2007; published online September 20, 2007)

Single carbon nanofibers (CNFs) grown on the tips of scanning probe microscopy (SPM) cantilevers by Ar^+ irradiation attract much attention, because of their potential in the batch fabrication of CNF probes. Here, we first revealed their mechanical characteristics. An excellent flexibility of CNF probes was confirmed by hard-contact examination (force-curve measurement) in which the cantilever was brought closer to the sample surface from a standard imaging position to a 300 nm-deeper position. Due to this flexibility and durability, even after continuous atomic force microscopy (AFM) imaging using a CNF probe (900 nm in length and 30 nm in diameter) for 200 min, no marked deterioration was observed in AFM resolution or probe shape. These mechanical properties of the ion-induced CNFs were comparable to those of high-quality carbon nanotube (CNT) probes. Therefore, it was concluded that CNF probes are promising as practical SPM probes.
[DOI: 10.1143/JJAP.46.6324]

KEYWORDS: scanning probe microscopy (SPM), atomic force microscopy (AFM), carbon nanofibers (CNFs), carbon nanotubes (CNTs)

1. Introduction

One-dimensional nanomaterials, such as carbon nanotubes (CNTs) and carbon nanofibers (CNFs), are thought to be an ideal probe for scanning probe microscopy (SPM), due to their possible high spatial resolution and suitability in measurements of high-aspect-ratio trenches and semiconductor patterns of narrow line-and-space.[1)] From the viewpoint of practical applications, on the other hand, SPM probes should possess sufficient lifetime and mechanical strength. For CNTs, their mechanical properties are known to depend on defect density. Excellent CNTs with no defect show the best mechanical properties.[2)] Thus, for CNT probes, the selection of defect-free CNTs is essential for better SPM imaging.

In a previous paper, we reported that single CNFs could be selectively grown onto commercial-type SPM tips using ion irradiation.[3)] In this method, the length and growth direction of CNFs are also controllable. Ion-induced CNFs have no hollow structure and are characterized by their amorphous nature.[4)] The amorphous nature implies that ion-induced CNFs possess no localized defect regions that cause structural deformation under mechanical stress. Thus, their mechanical properties may be superior to those of defect-rich CNTs, such as CNTs grown by chemical vapor deposition.[5–10)]

In this work, we tackled this interesting subject. The mechanical properties of ion-induced CNF probes were investigated in detail and compared with those of commercially available CNT and Si probes.

2. Experimental Methods

2.1 *Nanofabrication system*

The samples employed were commercially available SPM cantilevers. The basic fabrication of CNF probes is described elsewhere in detail.[3)] In brief, after coating a thin carbon layer onto the cantilevers, they were ion irradiated using a Kaufman-type ion gun, 3 cm in ion-source diameter, in a nanofabrication system.[4)] By ion irradiation, CNFs grow due to the redeposition of sputter-ejected carbon atoms onto the sidewall of conical protrusions and the excess surface diffusion of the carbon atoms to the tips during Ar^+ sputtering (Fig. 1).[3)] The Ar^+ ion beam energy employed for the ion-induced CNF growth was 600 eV, and the growth duration was about 10 min. The basal and working pressures

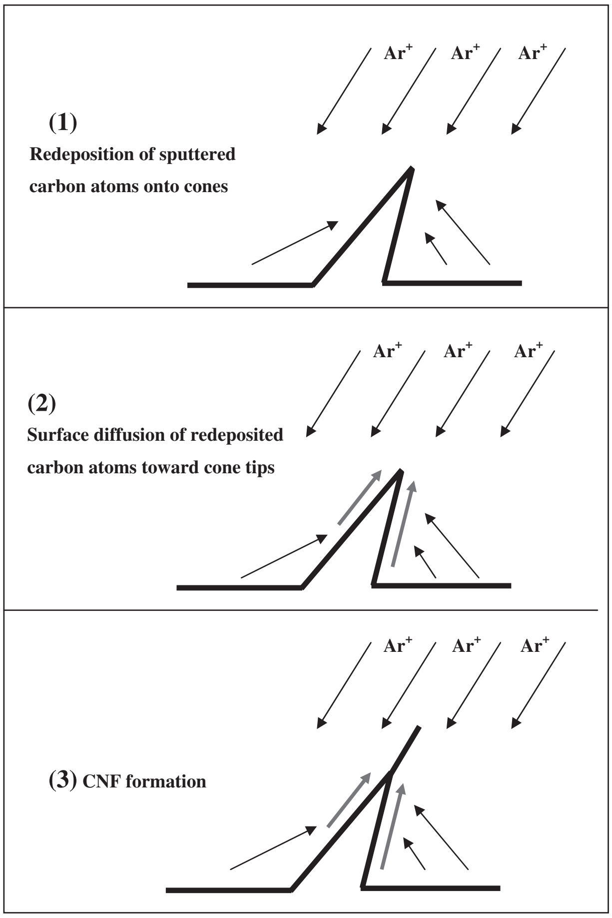

Fig. 1. Schematic representation of possible formation mechanism of CNFs by ion irradiation.

*E-mail address: ma_kitazawa@ot.olympus.co.jp

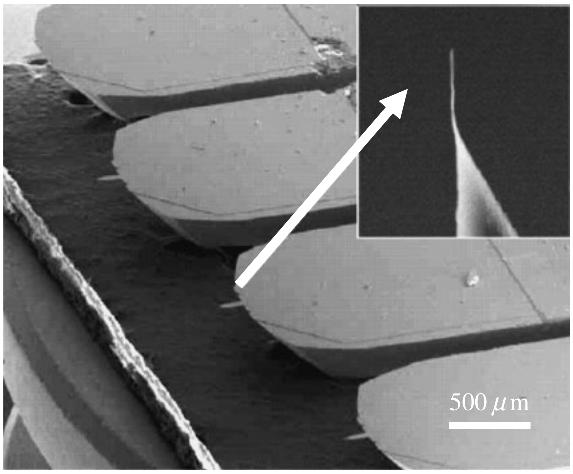

Fig. 2. SEM image of array of commercially available Si SPM cantilevers. Inset: Enlarged SEM image of ion-induced CNF grown on tip.

were 1.5×10^{-5} and 2×10^{-2} Pa, respectively. Several cantilevers were batch-processed to grow CNFs on their tips, as shown in Fig. 2.[11)]

2.2 Cantilever

Si Cantilevers employed for the CNF growth were commercially available tetrahedral types (Olympus OMCL-AC160TN, $L \times W \times T = 160 \times 50 \times 4.7\,\mu m^3$). Linear-shaped CNFs, 900 nm in length and 30 nm in diameter, were formed on these cantilevers by the above-described Ar^+ irradiation method. We also prepared two kinds of commercially available CNT probes for comparison of mechanical characteristics: (i) CNT-1 probe; a multiwall CNT synthesized by the arc discharge method was manually attached and glued onto a cantilever tip by electron-beam-induced carbon deposition under scanning electron microscopy (SEM) observation, and (ii) CNT-2 probe; a bundle of single-wall CNTs dispersed into a solvent was attached to a cantilever tip by an electrophoretic method. In general, CNTs generated by the arc discharge method and purified properly are known to be of high quality in terms of their crystalline structure. The manufacturing methods, mechanical characteristics, and sizes of the cantilevers (without CNT) are shown in Table I. Note that the resonance frequency of respective cantilevers is almost identical.

2.3 Evaluation

Force-curve measurements were carried out using an atomic force microscopy (AFM) machine (SII-NT E-Sweep). In this measurement, while the levers were brought closer to the surface at a constant speed from a normal imaging position of the sample to a 300-nm-deeper position, the dependence of the amplitude voltage of the lever (i.e., the cantilever deflection) on the displacement of the lever was recorded. Four kinds of cantilevers shown in Table I were examined. The probe shape was carefully observed by field-emission scanning electron microscopy (FESEM; Hitachi S-4700) before and after the force-curve measurements.

The durability of the probes was examined by 50 consecutive scans using AFM. In this examination, degradation in the image resolution was investigated after the 50th scan. The probe shape was also carefully observed by FESEM before and after the durability examination.

In the durability examination, a surface area of $5 \times 5\,\mu m^2$ of a standard titanium (Ti) sample (tip check sample, NT-MDT) was continuously scanned in the dynamic AFM scanning mode (Veeco D-3100). In this examination, the clearness of the Ti grain shape in the AFM image indicates the sharpness of the probe tip. The sharper the probe tip, the clearer the Ti grain shape in the AFM image. For the quantitative analysis of the sharpness of the probe tips, Tip Qualification software, D-3100, was used. The scan speed and the number of lines were set at 1 Hz and 256×256 lines, respectively. The examinations were carried out under heavy-loaded conditions. The examination time required was 200 min for the respective probes.

3. Results and Discussion

As for the first step of the mechanical characterization of the probes, we measured the force-curves for the respective probes. Since the mechanical characteristics of the lever parts are almost identical for the probes employed (see Table I), the inclination of the force-curve corresponds directly to the mechanical strength of the probe tip part that touches the surface of the sample. A small inclination of the

Table I. Manufacturing methods, characteristics, and sizes of cantilevers employed in this study.

Method	Ion-induced CNF	Manually attached CNT CNT-1	Electrophoretic CNT CNT-2	AC160T
Lever dimension $L \times W \times T$ (μm^3)	$160 \times 50 \times 4.7$	$125 \times 30 \times 3.6$	$150 \times 40 \times 3.8$	$160 \times 50 \times 4.7$
Resonance frequency (kHz)	265.1	255.3	257.8	267.9
Probe material	Amorphous CNF	CNT	CNT	Silicon
Si tip height (μm)	14	15	14	14
CNF/CNT height (μm)	0.9	0.3	2.5	—
Radius of curvature (nm)	15	11	21	7

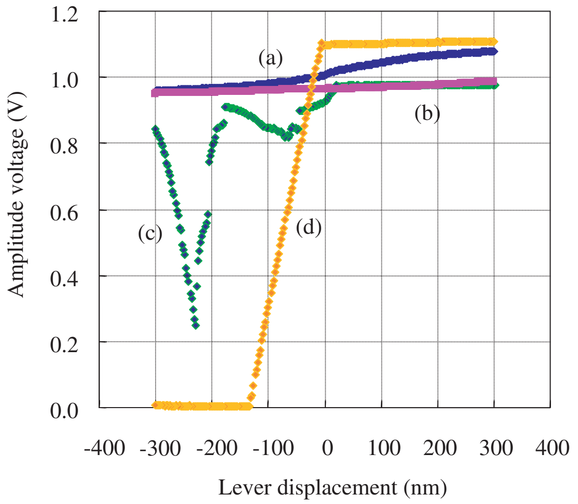

Fig. 3. Force-curve plot obtained for (a) CNF, (b) CNT-1, (c) CNT-2, and (d) Si probes.

force-curve implies that the change in amplitude voltage is small even for a large displacement of the lever. In other words, flexible probes yield a small inclination of the force curve.

Figure 3 shows the results of dynamic mode force-curve plots for the respective probes. The CNF (curve a) and CNT-1 (curve b) showed the same force-curve characteristics typical of flexible probes; the amplitude voltages decreased gradually with a decrease in the lever displacement at 0.1 and 0.06 mV/nm for the CNF and CNT-1 probes, respectively. By contrast, the Si probe (curve d) showed a force-curve characteristic typical of rigid probes; the amplitude voltages decreased steeply with a decrease in the lever displacement at 8.5 mV/nm and became zero when a lever displacement of about −130 nm was reached. The force-curve characteristic of CNT-2 (curve c) showed a complicated characteristic. This may be due to the plastic deformation of the CNT.

Figure 4 shows the SEM images of the probes after the force-curve measurements. No change in the probe shape was recognized for the CNF [Fig. 4(a)] and CNT-1 [Fig. 4(b)], proving that they possessed the elastic nature against the mechanical deflection. The gradual change in the amplitude voltage in the force-curve measurements would be due to this flexibility. By contrast, the probe was plastically deformed for CNT-2 [Fig. 4(c)] and the top part of the probe was broken and disappeared for the Si probe [Fig. 4(d)]. These fatal damages in the probe shape would be responsible for the sudden and marked change in the amplitude voltage in the force-curve measurements. For rod-shaped materials, the deflection is proportional to the cubes of length and inversely to the fourth power of the diameter of the rod. Thus, if the mechanical properties were identical for carbon probes, the deflection must have been the smallest for CNT-2 due to its diameter being the largest. Nevertheless, plastic deformation occurred only in CNT-2, suggesting its inferiority in terms of mechanical elasticity.

Figures 5(a) and 5(b) show AFM images of a Ti surface after the 1st and 50th scans in the durability test using a CNF probe, respectively. Since individual Ti grains were clearly distinguishable after the 50th scan [Fig. 5(b)], no marked

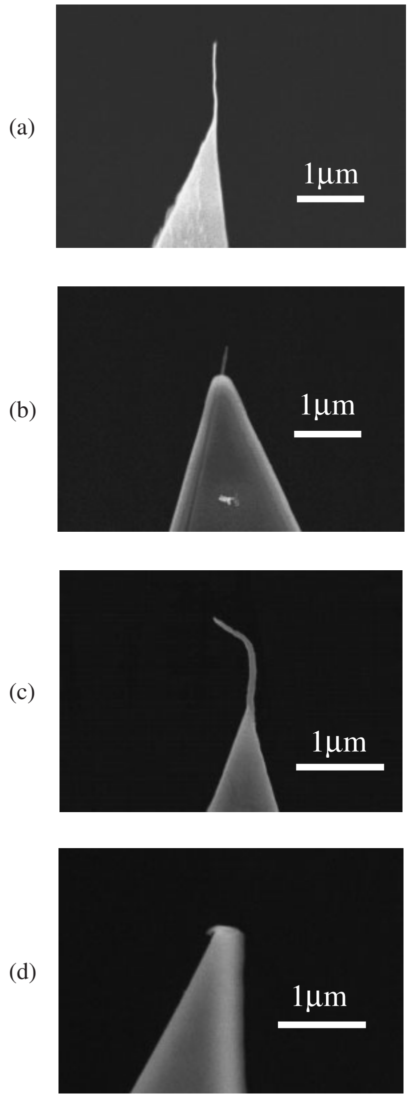

Fig. 4. SEM images of tips taken after force-curve measurement for (a) CNF, (b) CNT-1, (c) CNT-2, and (d) Si probes.

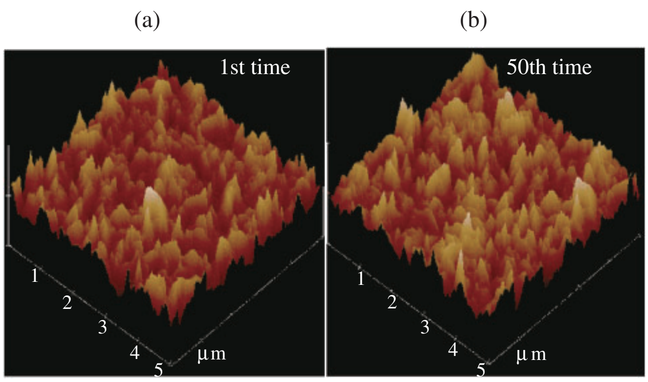

Fig. 5. AFM images of standard Ti sample surface obtained using CNF probe at (a) 1st and (b) 50th AFM scans.

degradation in the image resolution was recognizable after the durability examination. This was also confirmed by the qualitative analysis using Tip Qualification software [Fig. 6(a)]. The tip qualification analysis also revealed that the normalized radial curvature (i.e., the radial curvature of the tips normalized by the initial radial curvature) was quite

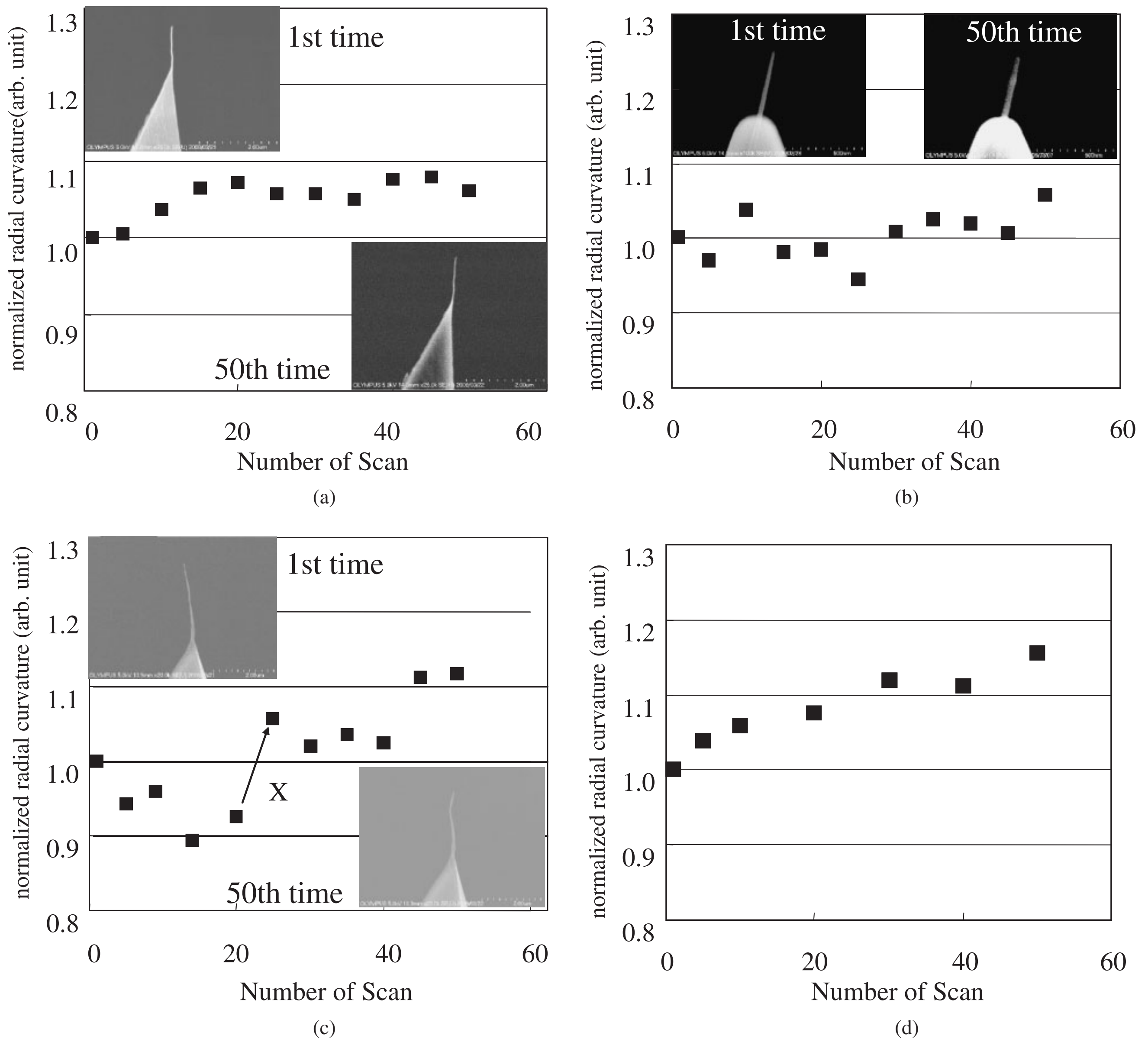

Fig. 6. Dependence of normalized radial curvature on number of scan attained for (a) CNF, (b) CNT-1, (c) CNT-2, and (d) Si probes. Insets: Enlarged FESEM images of tips taken before and after durability tests.

stable after several initial scans. Such stability in resolution is quite fascinating for practical use. The careful FESEM observations performed before and after the durability examination also showed no marked changes in the length, diameter, and shape of the CNF, as observed in the insets of Fig. 6(a).

The CNT-1 probe also showed excellent durability similarly to the CNF probe [Fig. 6(b)]. The deviation in the normalized radial curvature was about $\pm 5\%$. By contrast, a large degradation in the normalized radial curvature was detected for the CNT-2 probe [Fig. 6(c)]. The deviation in the normalized radial curvature reached about 20% or more. FESEM observations showed that the CNT was curved and shortened after the durability examination [insets of Fig. 6(c)]. These may be due to the localized defect in the CNT. A marked change in the normalized resolution observed at approximately the 20th scan [X in Fig. 6(c)] is thought to be attributed to the mechanical deformation of the CNT. Such a deformation may be due to the defect-rich structure of the CNT attached to the cantilever.

The scan-time dependence of the normalized radial curvature obtained for a conventional Si probe is shown in Fig. 6(d). The normalized radial curvature degraded gradually with scan time, and reached 1.16 after the 50th scan. This implies that the morphology (or curvature) of the probe tip changed during the scan. Figure 7 shows the FESEM images of the tip after the durability test, showing that a cotton-dustlike particle attached to the tip, and hence resulting in a duller tip. A Si probe is known to be contaminated readily with dustlike particles due to its hydrophilic nature. Note that cotton-dustlike particles were never observed after the durability tests for the carbon probes [see insets in Figs. 6(a)–6(c)]. The carbon probes were thought to be hardly contaminated during scans due to their hydrophobic nature. This implies that a long lifetime will be expected for carbon probes, being quite essential for practical applications.

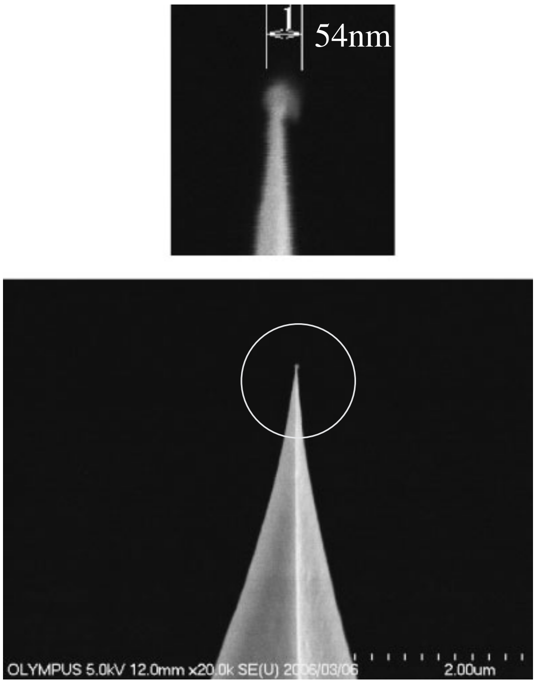

Fig. 7. SEM images of tips of silicon probe taken after 50th AFM scan. Upper part: Enlarged SEM image of tip.

4. Conclusions

The CNF probes were highly durable and flexible compared with the conventional Si probes. The mechanical properties of the CNF probes were almost identical to those of high-quality CNT probes, due to their amorphous nature that includes no localized defect region causing structural deformation under mechanical stress. Thus, it is considered that ion-induced CNF probes are promising as practical SPM probes.

Acknowledgements

This work was partly supported by the Japan Science and Technology Agency (JST), and the Japan Society for the Promotion of Science (JSPS), and a grant from the NITECH 21st Century COE Program "World Ceramics Center for Environmental Harmony".

1) S. Akita, H. Nishijima, Y. Nakayama, F. Tokumasu, and K. Takeyasu: J. Phys. D **32** (1999) 1044.
2) *Springer Handbook of Nanotechnology*, ed. B. Bhushan (Springer-Verlag, Berlin, 2003) Chap. 21.
3) M. Tanemura, M. Kitazawa, J. Tanaka, T. Okita, R. Ohta, L. Miao, and S. Tanemura: Jpn. J. Appl. Phys. **45** (2006) 2004.
4) M. Tanemura, J. Tanaka, K. Itoh, Y. Fujimoto, Y. Agawa, L. Miao, and S. Tanemura: Appl. Phys. Lett. **86** (2005) 113107.
5) J. H. Hafner, C. L. Cheung, and C. M. Lieber: Nature **398** (1999) 761.
6) J. H. Hafner, C. L. Cheung, and C. M. Lieber: J. Am. Chem. Soc. **121** (1999) 9750.
7) N. R. Franklin, Y. Li, R. J. Chen, A. Javey, and H. Dai: Appl. Phys. Lett. **79** (2001) 4571.
8) E. Yenilmez, Q. Wang, R. J. Chen, D. Wang, and H. Dai: Appl. Phys. Lett. **80** (2002) 2225.
9) P. M. Campbell, E. S. Snow, and J. P. Novak: Appl. Phys. Lett. **81** (2002) 4586.
10) Q. Ye, A. M. Cassell, H. Liu, K.-J. Chao, J. Han, and M. Meyyappan: Nano Lett. **4** (2004) 1301.
11) J. Tanaka, M. Kitazawa, M. Tanemura, and R. Ohta: to be published in J. Phys.: Conf. Ser. (2007).